Received: 15 January 2020 | Revised: 11 April 2020 | Accepted: 16 April 2020
DOI: 10.1111/cod.13563

ORIGINAL ARTICLE

CONTACT DERMATITIS WILEY

Optoacoustic mesoscopy shows potential to increase accuracy of allergy patch testing

Benedikt Hindelang[1,2,3] | Juan Aguirre[2,3] | Andrei Berezhnoi[2,3] | Hailong He[2,3] | Kilian Eyerich[1] | Vasilis Ntziachristos[2,3] | Tilo Biedermann[1] | Ulf Darsow[1]

[1]Department of Dermatology and Allergy, Faculty of Medicine, Technical University of Munich, Munich, Germany

[2]Chair of Biological Imaging and TranslaTUM, Technical University of Munich, Munich, Germany

[3]Institute of Biological and Medical Imaging, Helmholtz Zentrum München, Munich, Germany

Correspondence
Dr Benedikt Hindelang, MD, Department of Dermatology and Allergy, Technical University of Munich, Biedersteiner Strasse 29, 80802 Munich, Germany.
Email: benedikt.hindelang@tum.de

Dr Juan Aguirre, PhD, Chair of Biological Imaging, Technical University of Munich and Institute of Biological and Medical Imaging, Helmholtz Zentrum München, Neuherberg, Germany.
Email: juan.aguirre@helmholtz-muenchen.de

Abstract

Background: Differentiation between irritant and allergic skin reactions in epicutaneous patch testing is based largely on subjective clinical criteria, with the risk of high intraobserver and interobserver variability. Novel dermatological imaging using optoacoustic mesoscopy allows quantitative three-dimensional assessment of microvascular biomarkers.

Objectives: We investigated the potential of optoacoustic imaging to improve the precision of patch test evaluation.

Methods: Sixty-nine test reactions and 48 healthy skin sections in 52 patients with suspected type IV allergy were examined using raster-scan optoacoustic mesoscopy.

Results: We identified biomarkers from the optoacoustic images. Allergic reactions were associated with higher fragmentation of skin vasculature than irritant reactions (19.5 ± 9.7 vs 14.3 ± 3.7 fragments/100 pixels^2; $P < .05$), as well as lower ratio of low- to high-frequency acoustic signals (1.6 ± 0.5 vs 2.0 ± 0.6, $P < .05$). Allergic reactions graded "++" showed higher vessel fragmentation than reactions graded "+" (25.4 ± 13.2 vs 17.1 ± 6.5 fragments/100 pixels^2; $P < .05$). A linear model combining the biomarkers fragmentation and frequency ratio could differentiate allergic from irritant test reactions with an area under the receiving operator characteristic curve of 0.80 (95% confidence interval 0.64-0.91), reaching a sensitivity of 81% and specificity of 63%.

Conclusions: Optoacoustic mesoscopy shows potential to help in differentiating between allergic and irritant test reactions based on novel biomarkers that may reflect vasodilation, vessel tortuosity, and edema.

KEYWORDS

allergy, contact dermatitis, optoacoustic imaging, patch test, photoacoustic imaging

Abbreviations: ACD, allergic contact dermatitis; ICDRG, International Contact Dermatitis Research Group; MIP, maximum intensity projection; (HD-)OCT, (high-definition) optical coherence tomography; RCM, reflectance confocal microscopy; ROC, receiver operating characteristic; ROI, region of interest; RSOM, raster-scan optoacoustic mesoscopy; SLS, sodium lauryl sulfate.

This is an open access article under the terms of the Creative Commons Attribution License, which permits use, distribution and reproduction in any medium, provided the original work is properly cited.
© 2020 The Authors. Contact Dermatitis published by John Wiley & Sons Ltd.

1 | INTRODUCTION

Around 15% to 20% of the general population suffer from allergic contact dermatitis (ACD),[1] in which skin exposure to certain substances triggers innate and adaptive immune responses.[2,3] The disease presents as local dermatitis, which in some cases spreads to other parts of the skin. Affected individuals need to avoid the triggering substances for the rest of their lives.[3] The potentially long-term implications of an ACD diagnosis mean that this should be as accurate as possible. Epicutaneous patch testing constitutes the gold-standard diagnostic technique. The test substance is applied to the patient's skin, and then the clinician performs visual and palpatory assessment[4] to grade the skin response at 2 and 3 days or later. Severity of response is graded as 0, +, ++, or +++ in compliance with the recommendations of the ICDRG.[5] This test has at least three limitations. One is that clinical assessment is subjective and therefore subject to interphysician variation.[6] Another is that it distinguishes poorly between allergic skin reactions characteristic of ACD and irritant contact reactions arising when the test substance triggers cytotoxic effects on the skin.[2] Such irritant reactions are not indicators of underlying disorder, yet their misinterpretation as an allergic reaction can bring a misdiagnosis of ACD, with long-term consequences for the patient. A third limitation of the patch test is that it can give results that cannot be confidently assigned to allergic or irritant reactions. The ICDRG recommends rating such a reaction as doubtful positive (?+), with uncertain clinical implications for the patient.[7,8]

Objective complementary methods are needed to assist in the correct classification of epicutaneous patch test results. Histology can provide diagnostic clues in some cases. However, histology of allergic and irritant reactions can differ depending on the test substance, and skin reactions to a test substance have been shown to contain elements of both allergic and irritant reactions. Moreover, the invasiveness of skin biopsy makes histology unacceptable for routine use.[7,9] A number of noninvasive approaches have been suggested to help in the differentiation of allergic from irritant reactions.[10-13] Several trials have indicated the potential of reflectance confocal microscopy (RCM) and high-definition optical coherence tomography (HD-OCT) for identifying discriminatory biomarkers. In RCM imaging, allergic reactions present more epidermal vesicle formation while irritant reactions tend to show more pronounced disruption of the stratum corneum, more severe epidermal necrosis and parakeratosis, and stronger inflammatory infiltrate in superficial epidermal layers.[13-17] HD-OCT imaging also appears capable of resolving some of these features.[18]

However, RCM does not penetrate beyond approximately 300 μm, while HD-OCT does not penetrate beyond approximately 570 μm. In addition, they rely mainly on morphological rather than functional assessment of structures in the epidermis and superficial dermis, they offer small fields of view, and they cannot resolve the microvascular network. Moreover, vesicles are a feature of strong reactions which may need no imaging technique to be diagnosed clinically.

An imaging method capable of comprehensively assessing skin microvasculature may be beneficial for differentiating between allergic and irritant skin reactions. Results from colorimetry, laser Doppler flowmetry, and infrared thermography suggest that in mild irritant reactions, vasodilation may occur primarily in superficial dermal microvasculature, whereas allergic reactions may involve the global microvasculature.[19-21] Flow-sensitive dynamic OCT (D-OCT) is capable of imaging parts of the dermal microvasculature at high resolution. However, it is limited to an imaging depth of about 500 μm and, moreover, is affected by strong artifacts in the axial direction, which limits image analysis mostly to the en-face views.[22]

Raster-scan optoacoustic mesoscopy (RSOM) is a novel dermatological imaging method that can assess dermal microvasculature at high resolution.[22] In this technique, skin is illuminated with pulsed laser light that is absorbed by certain molecules in the skin, which generate ultrasound waves that are reconstructed into an image of the distribution of the absorbing molecules. Green laser light (532 nm) is absorbed nearly exclusively by melanin and hemoglobin, so the ultrasound waves generated can be reconstructed into three-dimensional (3D) images of the epidermal melanin layer and the comprehensive microvascular structure of the skin.[23-25] Using an ultrasound transducer with a central frequency of 55 MHz, RSOM can penetrate as deep as 1 to 1.5 mm and offers a resolution of about 8 μm in the axial dimension and 30 μm in the lateral dimension through the entire skin depth. When compared with D-OCT, RSOM thus offers a similar image quality in en-face images but allows for significantly better transverse cross-sectional images and a much greater penetration depth.

Overall, RSOM provides the highest resolution-to-depth ratio of all dermatological imaging techniques.[26] In pilot clinical studies, RSOM has been used to image psoriasis, where it enabled quantitative and objective assessment of inflammatory biomarkers as a measure of disease severity, and to image nailfold capillaries,[26,27] where it allowed measurement of biomarkers of systemic sclerosis in individuals whose cuticle was too thick to allow comprehensive assessment using conventional optical capillaroscopy.

We hypothesized that RSOM could be employed for routine examination of the microvascular structure in epicutaneous patch test reactions, and that this ability could contribute to a less subjective, more robust basis for differentiating between allergic and irritant patch test reactions.

In this exploratory study, we performed the first RSOM examination of allergic and irritant patch test reactions in patients undergoing routine epicutaneous patch testing, which we compared with RSOM analysis of healthy adjacent skin. We quantified objective vascular biomarkers and developed a linear discriminant model that was able to differentiate between allergic and irritant skin reactions. These results establish the potential of RSOM to improve the accuracy of patch testing, expanding the range of clinical contexts where the technique enables precision dermatology.

2 | METHODS

2.1 | Patients and patch test

The study protocol was approved by the Ethics Committee of the Faculty of Medicine of the Technical University of Munich. A total of 60 patients (38 women, 22 men; age range, 18-79 years; mean age, 51.8 years) participated in the study, after giving written informed consent. They were recruited among patients undergoing routine patch testing in the allergy unit of our university hospital. To be included in the study, patients had to be at least 18 years old and had to give a positive allergic skin reaction (+ or ++) to at least one of the 29 standard test substances recommended by the German Contact Dermatitis Research Group[28,29] and/or a positive reaction to sodium lauryl sulfate (SLS), which is recommended as an irritant control substance (SmartPractice Europe, Barsbüttel, Germany).[30] In general, recommendations of the European Society of Contact Dermatitis[31] were followed; however, substances were applied to the lateral and ventral upper arm in Finn Chambers (SmartPractice Europe, Barsbüttel, Germany) using Fixomull stretch patches (BSN medical, Hamburg, Germany). The substances remained on the skin for 48 hours. Then readings were taken on day (D) 2 after application (preliminary reading) and on D3 (definitive reading) by an experienced allergist trained in patch test assessment. Definitive readings were rated using the visual grading scale recommended by the ICDRG.[4]

2.2 | RSOM imaging system

The employed RSOM system was built in-house and equipped with an ultrasound transducer (Sonaxis, Besançon, France) detecting an ultra-broadband frequency range of 10 to 120 MHz and a central frequency of 55 MHz. The skin was illuminated using pulsed laser light (PI-Physik Instrumente, Karlsruhe, Germany) with a wavelength of 532 nm at a repetition rate of 500 Hz (Figure 1A). The detachable interface unit allowed precise positioning of the scan head on the skin surface (Figure 1B). A skin area of 4 × 2 mm was raster scanned for approximately 70 seconds. The system and its application have previously been described in detail.[24,26] Detected signals were separated into two frequency bands, typically 10 to 40 MHz and 40 to 120 MHz. The corresponding low-frequency band image (rendered in red color) and a high-frequency band image (rendered in green color) were reconstructed, frequency-equalized, and coregistered as described.[26] This operation allows simultaneous rendering of fine spatial details together with lower-resolution skin structures; the latter typically give more intense acoustic signal (Figure 1).[26]

2.3 | RSOM imaging of patch test reactions

In every patient, one allergic and/or one irritant reaction to SLS, and one adjacent nonmanipulated "healthy" skin region were imaged using RSOM, corresponding to 15 strong positive (++) allergic reactions, 40 weak positive (+) allergic reactions, 31 irritant reactions, and 57 healthy adjacent skin sections. Because of strong motion artifacts and technical malfunctions, 26 measurements (18.2%) were excluded. The final analysis included 13 ++, 31 +, and 25 irritant reactions, as well as 48 healthy adjacent skin sections from 52 patients.

2.4 | Quantitative evaluation of vascular features in different types of patch test reactions

For quantification, the following parameters were calculated from the imaging data: blood volume per skin surface, the high frequency-to-low frequency ratio, and vessel fragmentation. Prior to quantification, we applied a skin surface flattening algorithm to the images.[26] This enables proper quantification by separating the melanin layer from the microvascular tree.

2.4.1 | Width of vascularized dermis

The width of the vascularized dermis was determined as an average of five manual vertical measurements of the deepest dermal microvessel at different locations in the cross-sectional images (Figure 1C) obtained after performing a maximum intensity projection (MIP) in the sagittal direction. These measurements were performed by an analyst who was not one of the authors and who was blinded to applied test substances and to the results. The analyst was trained in interpreting RSOM images.

2.4.2 | Blood volume per surface and ratio of low- to high-frequency content

A 3D region of interest (ROI) was defined to calculate the blood volume per unit of surface area, the ratio of low- to high-frequency content, and vessel fragmentation. Selection of the ROI area was done by choosing a two-dimensional (2D) area (x and z) in the MIPs that encompassed the dermal vasculature down to a depth of 600 μm below the lower boundary of the epidermis. To define the 2D area, the lower boundary of the epidermis was marked manually in every image (upper dashed line in Figure 1C). The manual selection of the lower epidermal boundary to define the ROI was performed by a blinded analyst as described in section 2.5. Then, the 3D ROI was defined by extending the 2D area in the y dimension on the 3D reconstruction. We restricted ourselves to 600 μm below the lower epidermal boundary to ensure the highest possible image quality. Below 600 μm, artifacts may appear because the signal-to-noise ratio decreases, due to light attenuation with depth. Equalized reconstructions (R_{eq}) were generated following this expression: $R_{eq}=R_{low} + \alpha R_{high}$, *where* R_{low} is the low-frequency reconstruction, R_{high} is the high-frequency reconstruction, and α is the equalization parameter.[26] Then R_{eq} were used to calculate the blood volume per unit of skin surface

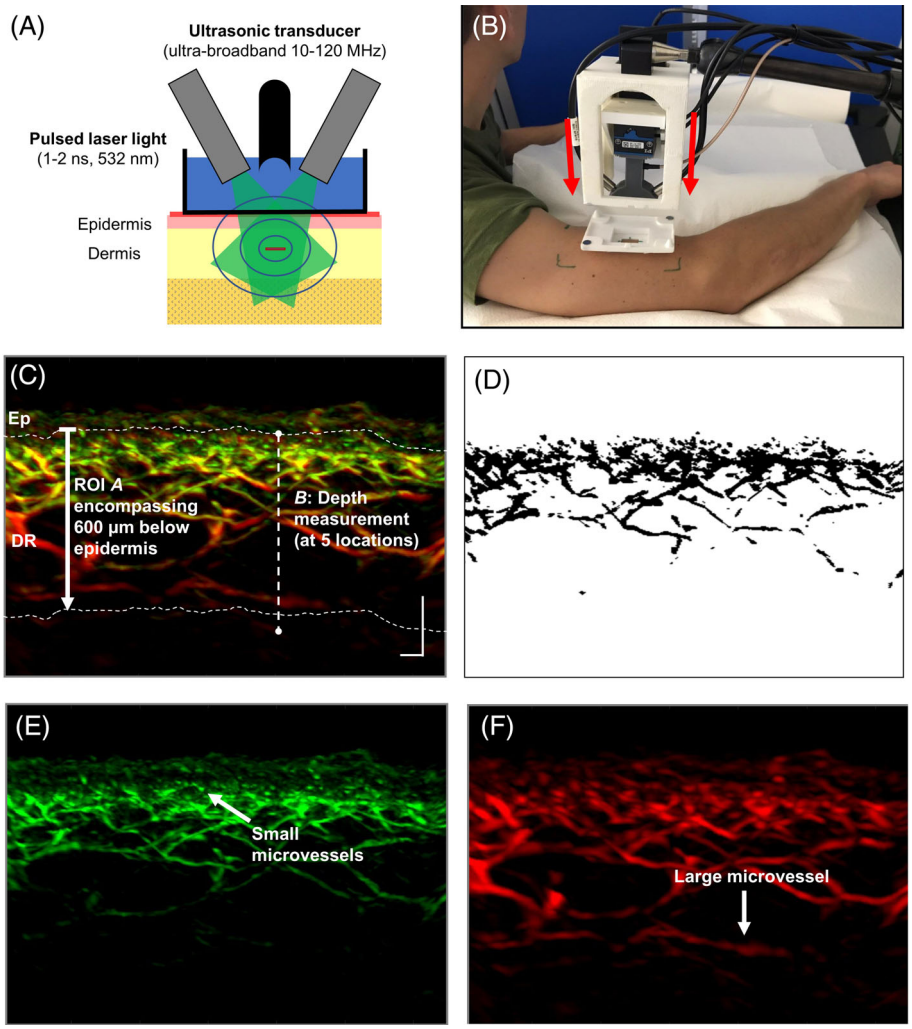

FIGURE 1 Illustration of the raster-scan optoacoustic mesoscopy (RSOM) system and quantification of RSOM images. (**A**) In RSOM imaging the skin is illuminated with pulsed laser light (green areas). Tissue chromophores, primarily hemoglobin and melanin, absorb the light and the tissue undergoes thermoelastic expansion. This produces ultrasound waves (blue concentric circles), which are detected by an ultra-broadband ultrasound transducer (black box) that is acoustically coupled to the skin via water. (**B**) For precise selection of the area to be imaged, a detachable interface is placed on the skin lesion. Subsequently, the RSOM scan head is mounted to the interface unit via magnets. (**C**) Cross-sectional maximum intensity projection of RSOM imaging data, including high-frequency content (green) and low-frequency content (red). The epidermis (Ep) and the microvasculature of the dermis (DR) are depicted. Blood volume per surface, ratio of low- to high-frequency content, and vessel fragmentation were quantified from the region of interest (ROI) *A*, encompassing the skin's microvasculature down to 600 µm below the lower boundary of the Ep (upper dashed line). The width of the vascularized DR was calculated as an average of five measurements. *B* constitutes an example measurement. (**D**) Binary black-and-white image of the high-frequency signal of the ROI *A* in panel C. Vessel fragmentation was determined from this image. (**E, F**) Cross sectional views of the same sample as in panel C showing only (E) high-frequency content or (F) low-frequency content. Smaller microvessels emit predominantly at high frequency, so they are preferentially visible in panel E, whereas larger microvessels emit at low frequency and dominate the field of view in panel F. The scale bars in panel C indicate 200 µm and apply to panels C-F

area, defined as BVS (µm) = (N × dV)/A, where N is the number of nonzero voxels after applying a 30% threshold to each equalized reconstruction, *dV* is the voxel volume, and *A* is the area of the skin surface situated above the selected ROI.

Using the same ROI, we calculated the blood volume as $BV = N \times dV$ separately for the low-frequency reconstruction and for the high-frequency reconstruction, after applying a threshold of 5% of the maximum voxel value for the low-frequency reconstruction and of 20% for the high-frequency reconstruction. The low- to high-frequency ratio was then defined as BV_{low}/BV_{high}, where BV_{low} and BV_{high} are, respectively, the low- and high-frequency blood volumes (Figure 1E,F).

2.4.3 | Vessel fragmentation

For determining the degree of vessel fragmentation, high-frequency ROI images from the sagittal MIP (discussed earlier) were transformed into a binary black-and-white image (Figure 1D) using the previously described threshold (20%). The number of vessel fragments contained

was quantified automatically using the image processing software ImageJ.[32] In particular, we used the menu command "Analyze Particles," which allows their size to be varied from zero to infinity and circularity from 0 (lines) to 1 (perfect circle). The number of vessel fragments was calculated per 100 × 100 pixels^2.

2.5 | Statistical analysis

The statistical significance of the differences found between the different types of patch test reactions and healthy skin was determined using the unpaired *t* test, Wilcoxon signed-rank test, and analysis of variance (ANOVA). In order to quantify the discriminative potential of RSOM to differentiate allergic from irritant reactions, we performed a linear discriminant analysis that included the two RSOM biomarkers of vessel fragmentation and ratio of low- to high-frequency content. The discriminant was trained using 29 allergic and irritant reactions, and then the resulting model was tested using the remaining 40 allergic and irritant reactions. The ability of these biomarkers to differentiate the two types of reaction was assessed in terms of the area under a receiver operating characteristic (ROC) curve, sensitivity, and specificity. Statistical tests were performed using MATLAB R2016b (MathWorks, Natick, Massachusetts), using a significance threshold of P_t = .05 (*t* test), P_w = .05 (Wilcoxon test) and P_{an} = .05 (ANOVA).

3 | RESULTS

3.1 | RSOM imaging of patch test reactions and healthy skin sections

Figure 2A-L show photographs and corresponding RSOM images of positive patch test reactions (irritant, + allergic, and ++ allergic) as well as adjacent healthy skin sections acquired in two patients. Figure 2A,G display photographs of healthy skin. Figure 2D, and Figure. 2J depict RSOM images of the respective skin sections. Below the clearly demarcated epidermal layer, the images show a dense superficial network of microvessels forming the subepidermal vascular plexus as well as deeper connecting vessels. Vessels appear continuous. Regarding the color-coded frequency content of the vasculature, which depends on vessel diameter, a pattern can be observed: the smaller microvessels of the superficial subepidermal plexus emit predominantly high-to-intermediate frequency signals (green to yellow), whereas larger, deeper connecting vessels emit lower frequencies (red). Figure 2B,H display

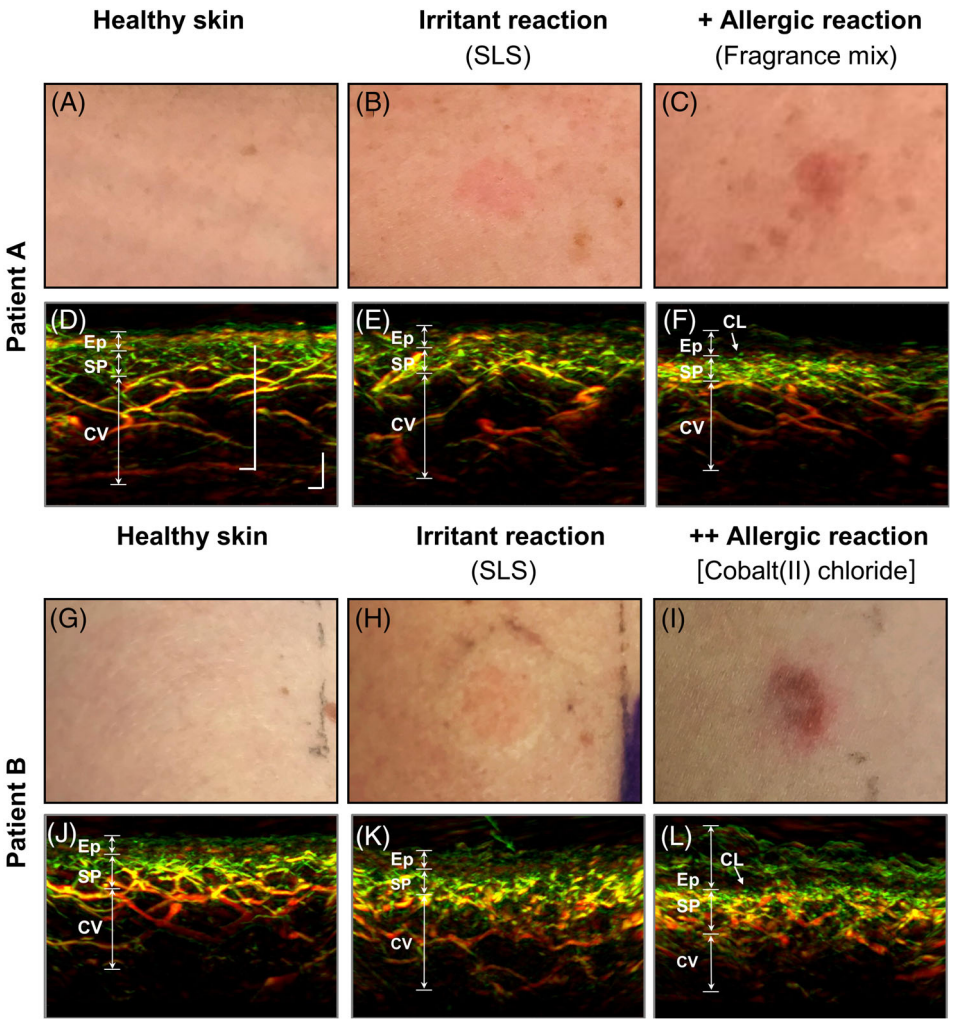

FIGURE 2 Raster-scan optoacoustic mesoscopy (RSOM) imaging of patch test reactions and healthy skin sections. (**A-C,G-I**) Photographs of healthy skin sections as well as irritant and allergic reactions in two patients. The irritant reactions were due to exposure to sodium lauryl sulfate (SLS), whereas the allergic reactions were due to fragrance mix and to cobalt (II) chloride, respectively. (**D-F, J-L**) Corresponding transversal cross-sectional RSOM images. Smaller microvessels emitting high-frequency ultrasound signals are depicted in green, and larger microvessels emitting low-frequency ultrasound signals are depicted in red. Intermediate frequency content is indicated in yellow. Both irritant and allergic reactions showed a less regular epidermis (Ep), vasodilation and fragmentation of the microvessels of the subepidermal plexus (SP) and connecting vessels (CVs), and greater dilation of capillary loops (CLs; arrow), which appear as green dots in these images. The scale bars in panel D represent 200 μm and apply to panels D-F and J-L

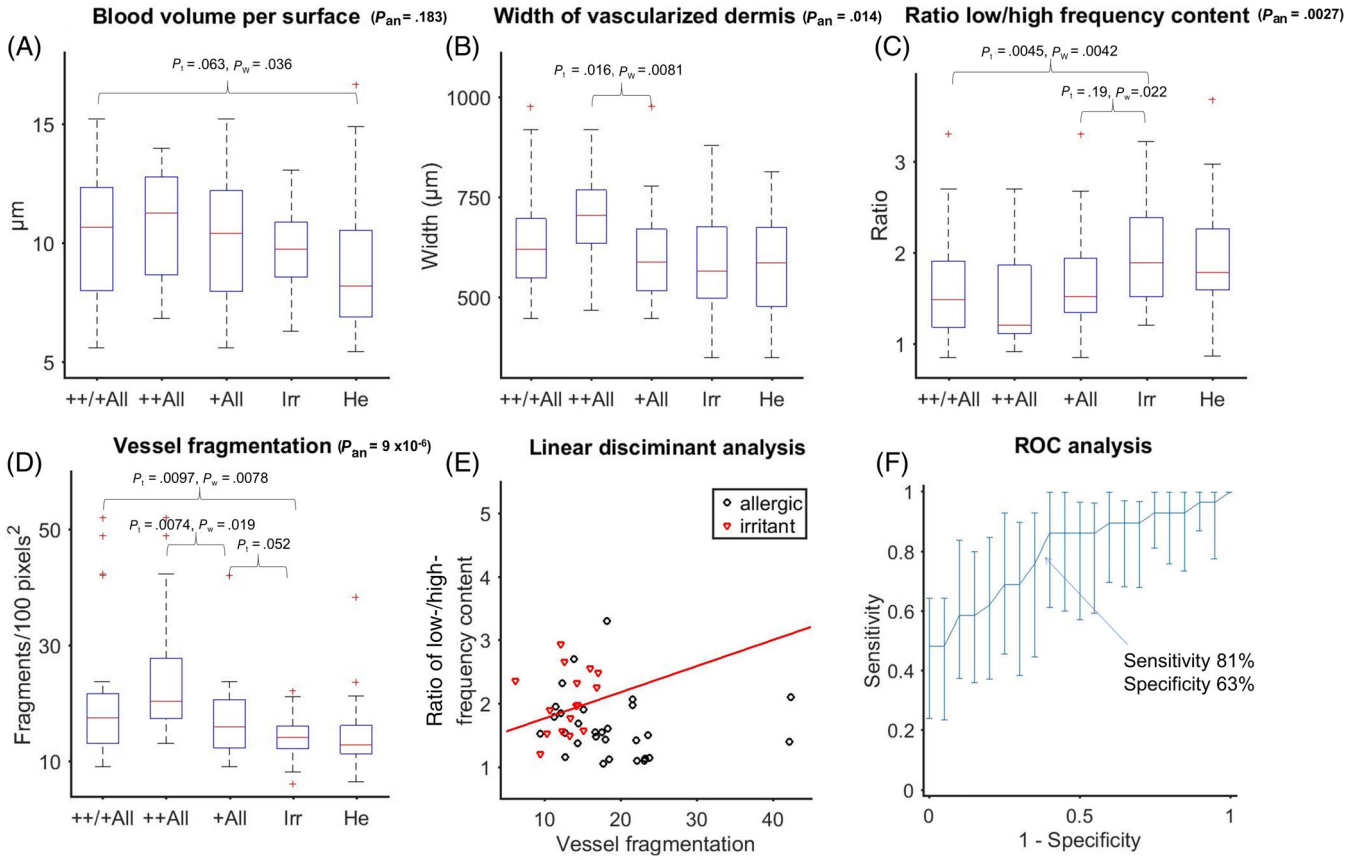

FIGURE 3 Quantitative analysis of raster-scan optoacoustic mesoscopy (RSOM) imaging of patch test reactions and healthy skin. (**A-D**) Box plots of RSOM biomarkers in patch test reactions and healthy skin. (**E**) Linear discriminant analysis in which the discriminant model calculated for the two biomarkers of low- to high-frequency content ratio and vessel fragmentation in the training data has been applied to the test data. The individual dots represent reactions to allergen or irritant test substances. (**F**) Receiver operating characteristic (ROC) curve analysis of the discriminatory potential of the linear discriminant model in panel E when applied to the test data. All, allergic reaction; He, healthy skin; Irr, irritant reaction; P_t, t test; P_w, Wilcoxon test; P_{an}, analysis of variance test

photographs of irritant reactions to SLS. They show mild but clearly delineated erythema. Figure 2E,K depict the corresponding RSOM images, and they reveal a less regular epidermal layer and vasodilation relative to healthy skin. They also indicate denser vasculature containing a larger number of discontinuous patchy areas, in particular in the subepidermal plexus. Figure 2C,F depict an + allergic patch test reaction to fragrance mix. The photograph (Figure 2C) shows a delineated erythema, which was associated with mild infiltration based on palpatory assessment. The corresponding RSOM image (Figure 2F) shows a thin, irregular epidermis and a denser, more dilated vascular network in the subepidermal plexus than in the irritant reaction. Figure 2I,L shows a ++ allergic reaction to cobalt(II) chloride. The photograph (Figure 2I) shows strong erythema and papules, which were associated with palpable infiltration. The corresponding RSOM image (Figure 2L) shows a much more irregular epidermal layer, greater vasodilation, and more discontinuous vessels than in the irritant or + allergic reactions. Tips of dilated capillary loops, which appear as green dots in the RSOM images, are more visible and contribute to a more discontinuous appearance of the microvascular structure in allergic reactions than in irritant reactions.

3.2 | Quantification of optoacoustic biomarkers in patch test reactions

Of major importance for our study was the identification of optoacoustic biomarkers in allergic and irritant contact dermatitis. The biomarker blood volume per skin surface area was quantified from the dermal microvasculature within 600 µm beneath the epidermis. The width of the vascularized dermis was calculated as the average depth of the deepest dermal microvessels at five locations of a scan area (Figure 1C). Moreover, we measured the ratio of low- to high-frequency content, where the low-frequency signal corresponds to larger microvessels and the high-frequency signal corresponds to smaller microvessels (Figure 1E,F). The fourth biomarker which we identified was vessel fragmentation, defined as an index of vessel fragments quantified from a binary black and white image of each data set's MIP (Figure 1D).

Figure 3 depicts box plots comparing the distribution of different optoacoustic biomarkers in positive patch test reactions (irritant, + allergic, and ++ allergic) and adjacent healthy skin. Figure 3A shows no statistically significant differences in blood volume-to-

surface area ratio among the three types of skin regions for both the *t* test and the Wilcoxon test. Nevertheless, there was a tendency for allergic reactions (+ and ++) to contain a higher blood volume than healthy skin (10.7 ± 3.3 μm vs 9.3 ± 3.7 μm; P_t = .063, P_w = .036). The ANOVA test showed no statistically significant difference between groups (P_{an} = .18). Figure 3B shows that the width of vascularized dermis in ++ allergic reactions was higher than in + allergic reactions (702 ± 116 μm vs 598 ± 129 μm; P_t = .016, P_w = .0081); additionally, the ANOVA test indicates that not all the groups may have the same mean value (P_{an} = .014). Figure 3C shows that the ratio of low- to high-frequency content was significantly lower in allergic reactions (+ and ++) than in irritant reactions (1.6 ± 0.5 vs 2.0 ± 0.6; P_t = .0045 and P_w = .0042), as well as significantly lower in + allergic reactions than in irritant reactions (1.7 ± 0.5 vs 2.0 ± 0.6; P_t = .019 and P_w = .022). Overall, the ANOVA test suggests that not all of the groups are equal (P_{an} = .0027). Figure 3D shows that allergic reactions (+ and ++) had a significantly higher number of vessel fragments than irritant reactions (19.5 ± 9.7 vs 14.3 ± 3.7 fragments per 100 pixels^2; P_t = .0097, P_w = .0078). The difference in the number of vessel fragments between irritant and + allergic reactions was borderline significant according to *t* test (*P* = .052) and not significant according to Wilcoxon test. The number of vessel fragments was significantly higher in ++ allergic reactions than in + allergic reactions (25.4 ± 13.2 vs 17.1 ± 6.5 fragments per 100 pixels^2, P_t = .0074, P_w = .007), whereas the ANOVA test suggests a clear difference between groups (P_{an} < .0001). Following the results of the previous statistical tests, we developed a linear discriminant model to differentiate between allergic and irritant reactions based on the ratio of low- to high-frequency content and vessel fragmentation. Figure 3E shows the application of that model to the test data comprising 45 allergic (+ and ++) and irritant reactions. Figure 3F assesses the ability of the linear discriminant model to different between allergic and irritant reactions in terms of the area under the ROC curve, sensitivity, and specificity. The area under the ROC curve was 0.80 (95% confidence interval [CI] 0.64-0.91) and the optimal cut-off value gave sensitivity of 81% and specificity of 63%.

4 | DISCUSSION

This is the first report on the use of RSOM in allergy diagnosis. The study demonstrates that RSOM is suitable for imaging patch test reactions in a clinical setting and that its unique ability to resolve skin microvasculature comprehensively enables the analysis of novel biomarkers that may increase the accuracy of interpreting patch test results. Here we provide evidence that two biomarkers in particular, vessel fragmentation and ratio of low- to high-frequency content, may differ significantly between allergic and irritant results, allowing more accurate assessment. Considering the high prevalence of contact allergies in the general population and the shortcomings of current patch test reading, our findings have important implications for precision allergology.

We found that allergic reactions were associated with significantly lower ratio of low- to high-frequency ultrasound content emitted by the dermal microvessels and higher vessel fragmentation than irritant reactions. These differences were also observed specifically between + allergic reactions and irritant reactions. High-frequency optoacoustic signal is emitted mainly by smaller microvessels, in particular the capillary loops of the papillary dermis.[25,26] The greater proportion of high-frequency content in the images corresponding to allergic reactions reflects a higher degree of vasodilation in smaller vessels such as the capillary loops, which is observed in many of the RSOM images in the present study. Our results are in line with histology studies, which have found stronger vasodilation in particular in the small capillaries of the papillary dermis in allergic when compared with irritant reactions.[7] The higher degree of vessel fragmentation in allergic reactions is most likely associated with increased vessel tortuosity, dermal edema, and possibly extravasation of erythrocytes. Because of the numerical aperture of the ultrasound transducer, structures oriented perpendicular to the skin surface cannot be resolved by RSOM. Therefore, vessels with such orientations are only partially visualized and appear patchy or fragmented. This effect has previously been described in clinical RSOM studies of psoriatic skin[26] and nailfold capillaries[27] and was confirmed by histologic observations.[26] Tortuous vessels are more likely to have sections running perpendicular to the skin surface that therefore appear fragmented in RSOM. Increased microvessel tortuosity may be associated with vasodilation and microvascular congestion, which are found in histologic assessments of allergic patch test reactions.[7] Dermal edema, well known to be more characteristic of allergic reactions than irritant reactions,[7] may constitute an additional factor changing the geometrical configuration of the skin's microvasculature and increasing the level of vessel fragmentation in RSOM imaging. Extravasation of erythrocytes occurs occasionally in allergic reactions,[7] and this could also help explain the frequent appearance of patchy structures in RSOM images of allergic reactions, because optoacoustic imaging cannot distinguish intravascular and extravascular hemoglobin.

The study also found significant differences between + allergic and ++ allergic reactions regarding the biomarkers vessel fragmentation and width of the vascularized dermis. Stronger vessel fragmentation in ++ allergic reactions most likely reflects an increasing degree of vessel tortuosity, dermal edema, and possibly erythrocyte extravasation when allergic reactions are stronger. The greater width of the vascularized dermis can be explained by swelling of the dermis as a result of edema. Our results suggest that RSOM may serve as an appropriate tool contributing to more objective grading of allergic patch test reactions.

Existing dermatological imaging methods, such as confocal microscopy, OCT, and laser Doppler flowmetry, do not allow comprehensive morphological analysis of skin microvasculature. Therefore, it is not possible to compare most of our results with such methods. Nevertheless, studies that quantified dermal blood flow using Laser Doppler devices did not find significant differences between allergic and irritant reactions.[21,33,34] This is in line with our finding that distribution of blood volume, which strongly depends on blood flow,[24,35]

did not differ significantly between the types of skin reactions. Comparison of laser Doppler and colorimetry analyses led to a suggestion that mild irritant reactions might be associated with more superficial vasodilation,[19,21] but our direct observation of microvessels in this study did not confirm this (data not shown).

ROC analysis showed that a linear discriminant model including the biomarkers of ratio of low- to high-frequency content and vessel fragmentation showed promising results regarding the discrimination of allergic and irritant reactions (area under the ROC curve 0.80; 95% CI 0.64-0.91). This result demonstrates the potential of optoacoustic imaging as a diagnostic device in the clinic. So far, the model has, however, only been applied to clear-cut allergic and irritant reactions. Analyzing a larger set of doubtful reactions in subsequent studies should allow a more comprehensive assessment of the usefulness of this approach.

This is the first study to apply optoacoustic imaging to the assessment of dermal microvascular reactions in allergy patch testing. The results suggest that the noninvasive technique can identify quantitative biomarkers that can differentiate between allergic and irritant reactions. Future studies should verify and extend our results, which will require overcoming certain technical challenges. The quality of the imaging data in our study varied considerably from one skin scan to the next. Slight motion artifacts were common, reflecting the proximity between the tested upper arm area and the torso, which moves with breathing.[36] This led us toward indirect quantitative analysis of the data assessing frequency content and fragmentation of microvasculature, and away from determination of individual vessel diameters. RSOM is likely to become faster, and the resulting shorter scan times will reduce susceptibility to motion artifacts such as movements of the patient, ultimately allowing even more detailed evaluation. Automatic segmentation and analysis algorithms, which have been implemented in other imaging methods[37,38] and have also already helped in evaluating RSOM data,[26] should make this evaluation easier in the future.

This study demonstrates that RSOM imaging can be used for high-resolution imaging of skin allergic reactions. As a complementary diagnostic measure, potentially as a score in combination with clinical features, it holds potential to increase the precision of allergy patch testing, which can improve the diagnosis and management of individuals affected by contact dermatitis.

ACKNOWLEDGEMENTS

This project received funding from the European Union's Horizon 2020 Research and Innovation Programme (grant agreement number 687866 [INNODERM]), from the European Research Council (ERC) under the European Union's Horizon 2020 Research and Innovation Programme (grant agreement number 694968 [PREMSOT]), and from Deutsche Forschungsgemeinschaft (DFG; grant agreement number SFB 824, project B10).

CONFLICTS OF INTEREST

V.N. has a financial interest in iThera Medical GmbH, Munich, Germany, which, however, was not involved in this work. The other authors declare no conflicts of interest.

ORCID

Benedikt Hindelang https://orcid.org/0000-0003-4350-0518

REFERENCES

1. Thyssen JP, Linneberg A, Menné T, Johansen JD. The epidemiology of contact allergy in the general population--prevalence and main findings. *Contact Dermatitis*. 2007;57(5):287-299.
2. Martin SF. Contact dermatitis: from pathomechanisms to immunotoxicology. *Exp Dermatol*. 2012;21(5):382-389.
3. Rustemeyer T, van Hoogstraten IM, von Blomberg BME, Scheper RJ, Frosch PJ, Menné T, Lepoittevin J-P. Mechanisms in Allergic Contact Dermatitis eds. *Contact Dermatitis*. Berlin, Germany: Springer Berlin Heidelberg; 2006.
4. Lachapelle J-M, Maibach HI. *Patch Testing and Prick Testing: A Practical Guide Official Publication of the ICDRG*. 3rd ed.Berlin, Germany: Springer Berlin Heidelberg; 2012:2012.
5. Wilkinson DS, Fregert S, Magnusson B, et al. Terminology of contact dermatitis. *Acta Derm Venereol*. 1970;50(4):287-292.
6. Svedman C, Isaksson M, Björk J, Mowitz M, Bruze M. Calibration' of our patch test reading technique is necessary. *Contact Dermatitis*. 2012;66(4):180-187.
7. Lachapelle J-M, Marot L. Histopathological and immunohistopathological features of irritant and allergic contact dermatitis. In: Frosch PJ, Menné T, Lepoittevin J-P, eds. *Contact Dermatitis*. Berlin, Germany: Springer Berlin Heidelberg; 2006:107-116.
8. Davis MDP, Yiannias JA. Should macular erythema reactions be counted as positive allergic patch-test reactions? *Dermatitis*. 2006;17(1):12-14.
9. Vestergaard L, Clemmensen OJ, Sørensen FB, Andersen KE. Histological distinction between early allergic and irritant patch test reactions: follicular spongiosis may be characteristic of early allergic contact dermatitis. *Contact Dermatitis*. 1999;41(4):207-210.
10. Serup J, Stabero B. Ultrasound for assessment of allergic and irritant patch test reactions. *Contact Dermatitis*. 1987;17(2):80-84.
11. Ermolli M, Menné C, Pozzi G, Serra MA, Clerici LA. Nickel, cobalt and chromium-induced cytotoxicity and intracellular accumulation in human hacat keratinocytes. *Toxicology*. 2001;159(1–2):23-31.
12. Gambichler T, Moussa G, Sand M, et al. Correlation between clinical scoring of allergic patch test reactions and optical coherence tomography. *J Biomed Opt*. 2005;10(6):64030.
13. Sakanashi EN, Matsumura M, Kikuchi K, Ikeda M, Miura H. A comparative study of allergic contact dermatitis by patch test versus reflectance confocal laser microscopy, with nickel and cobalt. *Eur J Dermatol*. 2010;20(6):705-711.
14. Bohaty B, Fricker C, González S, Gill M, Nedorost S. Visual and confocal microscopic interpretation of patch tests to benzethonium chloride and benzalkonium chloride. *Skin Res Technol*. 2012;18(3):272-277.
15. Slodownik D, Levi A, Lapidoth M, Ingber A, Horev L, Enk CD. Noninvasive in vivo confocal laser scanning microscopy is effective in differentiating allergic from nonallergic equivocal patch test reactions. *Lasers Med Sci*. 2015;30(3):1081-1087.
16. Astner S, González E, Cheung AC, et al. Non-invasive evaluation of the kinetics of allergic and irritant contact dermatitis. *J Invest Dermatol*. 2005;124(2):351-359.
17. Astner S, González S, Gonzalez E. Noninvasive evaluation of allergic and irritant contact dermatitis by in vivo reflectance confocal microscopy. *Dermatitis*. 2006;17(4):182-191.
18. Boone MALM, Jemec GBE, Del Marmol V. Differentiating allergic and irritant contact dermatitis by high-definition optical coherence tomography. *Arch Dermatol Res*. 2015;307(1):11-22.
19. Agache P. Assessment of erythema and pallor. In: Humbert P, Fanian F, Maibach HI, Agache A, eds. *Agache's Measuring the Skin:*

Non-invasive Investigations, Physiology, Normal Constants. 2nd ed. ; 2017:1367-1377.
20. Baillie AJ, Biagioni PA, Forsyth A, Garioch JJ, McPherson D. Thermographic assessment of patch-test responses. *Br J Dermatol*. 1990;122 (3):351-360.
21. Gawkrodger DJ, McDonagh AJG, Wright AL. Quantification of allergic and irritant patch test reactions using laser-Doppler flowmetry and erythema index. *Contact Dermatitis*. 1991;24(3):172-177.
22. Hindelang B, Aguirre J, Schwarz M, et al. Non-invasive imaging in dermatology and the unique potential of raster-scan optoacoustic mesoscopy. *J Eur Acad Dermatol Venereol*. 2018;33(6):1051-1061.
23. Aguirre J, Schwarz M, Soliman D, Buehler A, Omar M, Ntziachristos V. Broadband mesoscopic optoacoustic tomography reveals skin layers. *Opt Lett*. 2014;39(21):6297-6300. https://doi.org/10.1364/OL.39.006297
24. Berezhnoi A, Schwarz M, Buehler A, Ovsepian S, Aguirre J, Ntziachristos V. Assessing hyperthermia-induced vasodilation in human skin in vivo using optoacoustic mesoscopy. *Journal of Biophotonics*. 2018;11(11):e201700359. http://dx.doi.org/10.1002/jbio.201700359
25. Schwarz M, Omar M, Buehler A, Aguirre J, Ntziachristos V. Implications of ultrasound frequency in optoacoustic mesoscopy of the skin. *IEEE Trans Med Imaging*. 2015;34(2):672-677.
26. Aguirre J, Schwarz M, Garzorz N, et al. Precision assessment of label-free psoriasis biomarkers with ultra-broadband optoacoustic mesoscopy. *Nat Biomed Eng*. 2017;1(5):68.
27. Aguirre J, Hindelang B, Berezhnoi A, et al. Assessing nailfold microvascular structure with ultra-wideband raster-scan optoacoustic mesoscopy. *Photoacoustics*. 2018;10:31-37.
28. Mahler V, Geier J, Schnuch A. Current trends in patch testing - new data from the German contact dermatitis research group (DKG) and the information network of departments of dermatology (IVDK). *J Dtsch Dermatol Ges*. 2014;12(7):583-592.
29. Deutsche Kontaktallergiegruppe. Epikutantestreihen der DKG. https://dkg.ivdk.org/testreihen.html. Accessed February 24, 2019.
30. Schnuch A, Aberer W, Agathos M, et al. Durchführung des Epikutantests mit Kontaktallergenen. *J Dtsch Dermatol Ges*. 2008;6(9):770-775.
31. Johansen JD, Aalto-Korte K, Agner T, et al. European Society of Contact Dermatitis guideline for diagnostic patch testing - recommendations on best practice. *Contact Dermatitis*. 2015;73(4):195-221.
32. Schneider CA, Rasband WS, Eliceiri KW. NIH image to ImageJ: 25 years of image analysis. *Nat Methods*. 2012;9(7):671-675.
33. Goon AT-J, Leow Y-H, Chan Y-H, Goh C-L. Correlation between laser Doppler perfusion imaging and visual scoring of patch test sites in subjects with experimentally induced allergic and irritant contact reactions. *Skin Res Technol*. 2004;10(1):64-66.
34. Staberg B, Serup J. Allergic and irritant skin reactions evaluated by laser Doppler flowmetry. *Contact Dermatitis*. 1988;18(1):40-45.
35. Prothero JW, Burton AC. The physics of blood flow in Capillaires: II. The capillary resistance to flow. *Biophys J*. 1962;2(2 Pt 1):199-212.
36. Aguirre J, Berezhnoi A, He H, et al. Motion quantification and automated correction in clinical RSOM. *IEEE Trans Med Imaging*. 2019;38 (6):1340-1346.
37. Bulant CA, Blanco PJ, Müller LO, Scharfstein J, Svensjö E. Computer-aided quantification of microvascular networks: application to alterations due to pathological angiogenesis in the hamster. *Microvasc Res*. 2017;112:53-64.
38. Yousefi S, Liu T, Wang RK. Segmentation and quantification of blood vessels for OCT-based micro-angiograms using hybrid shape/intensity compounding. *Microvasc Res*. 2015;97:37-46.

How to cite this article: Hindelang B, Aguirre J, Berezhnoi A, et al. Optoacoustic mesoscopy shows potential to increase accuracy of allergy patch testing. *Contact Dermatitis*. 2020; 1–9. https://doi.org/10.1111/cod.13563